Synthesis and Electrochemical Characteristics of $Li_{0.7}[Ni_{0.05}Mn_{0.95}]O_2$ as a Positive Material for Rechargeable Lithium Batteries

Sun-Sik Shin, Dong-Won Kim,† and Yang-Kook Sun*

Department of Chemical Engineering, Hanyang University, Seoul 133-791, Korea
†Department of Chemical Technology, Hanbat National University, Taejon 305-719, Korea
Received September 18, 2001

Layered $Na_{0.7}[Ni_{0.05}Mn_{0.95}]O_2$ compounds have been synthesized by a sol-gel method, using glycolic acid as a chelating agent. $Na_{0.7}[Ni_{0.05}Mn_{0.95}]O_2$ precursors were used to prepare layered lithium manganese oxides by ion exchange for Na by Li, using LiBr in hexanol. Powder X-ray diffraction shows the layered $Li_{0.7}[Ni_{0.05}Mn_{0.95}]O_2$ has an O3 type structure, which exhibits a large reversible capacity of approximately 190 mA h g^{-1} in the 2.4-4.5 V range. $Li_{0.7}[Ni_{0.05}Mn_{0.95}]O_2$ powders undergo transformation to spinel during cycling.

Keywords : Lithium secondary batteries, Sol-gel method, Layered manganese, Cathode materials.

Introduction

Commercialized lithium-ion batteries use layer structured $LiCoO_2$ cathodes. Because of the high cost and toxicity of cobalt, an intensive search for new cathode materials has been underway in recent years. One of the most attractive cathode materials are the spinel $LiMn_2O_4$ and its derivatives due to their low cost, abundance, and nontoxicity.[1-5] However, the spinel $LiMn_2O_4$ and its derivatives demonstrate smaller discharge capacity than layer structured materials and a slow capacity loss at elevated temperature in the range of 50-80 °C.[6-9] Therefore, researchers have studied the preparation of layered $LiMnO_2$ with the O3 (α-$NaFeO_2$) structure as $LiCoO_2$ and $LiNiO_2$. Direct synthesis of O3 $LiMnO_2$ is not possible because the non-layered structures $LiMn_2O_4$ (spinel), $LiMnO_2$ (orthorhombic), or Li_2MnO_3 (rock salt) are more stable at high temperature. Monoclinic $LiMnO_2$ (m-$LiMnO_2$) with the layered rock salt structure (α-$NaFeO_2$ type) has been synthesized by ion exchange of lithium salts with $NaMnO_2$, but significant loss has been reported at room temperature though the initial capacity is high.[10-12] Stoichiometric $LiMnO_2$ converts to the stable spinel-like phase by minor cationic rearrangements during cycling, leading to degradation of electrode performance.

According to a phase diagram of Na_xMnO_2 developed by Parant *et al*., $Na_{0.7}MnO_2$ exists in two different phases, the oxygen-rich stoichiometry α-$Li_{0.7}MnO_{2+y}$ ($0.05 < y < 0.25$) and β-$Li_{0.7}MnO_{2+y}$ ($y < 0.05$). The α-$Li_{0.7}MnO_{2+y}$ is stable below at 600 °C and has hexagonal P2 structure, while high-temperature β-$Li_{0.7}MnO_{2+y}$ has an orthorhombic-distorted P2 structure.[13] Recently, Paulsen *et al.* reported that the high temperature O2-type $Li_{0.7}Ni_{1/3}Mn_{2/3}O_2$ prepared by ion exchange Li for Na from the P2-type $Na_{0.7}Ni_{1/3}Mn_{2/3}O_2$ showed a large capacity of about 180 mAh/g and good capacity retention.[14-16] Although they prepared a very pure low-temperature O3-type $Li_{0.7}MnO_{2+y}$ phase, the material converts gradually to spinel by the evolution of plateaus at 3 and 4 V.

In the present study, a sol-gel method was employed to prepare layered $Li_{0.7}[Ni_{0.05}Mn_{0.95}]O_2$ powders, using glycolic acid ($HOCH_2COOH$) as a chelating agent at the low temperature condition. The dissociation constant and water solubility of the glycolic acid is 3.83 and 1E+006 mg/L (at 25 °C), respectively. The sol-gel method, one of the solution methods, has many advantages, such as good stoichmetric control and production of active submicro-size particles in a relatively shorter processing time at a relatively lower temperature, compared with manufacturing methods that use by the conventional solid- state reaction. Another advantage is the association of the solid colloidal state with a liquid medium, thus avoiding any pollution by eventual dispersion of dust.[17] The structural and electrochemical properties of the materials are investigated using various analytical techniques and correlated to explain the electrochemical properties of the materials.

Experimental Section

Samples of $Na_{0.7}[Ni_{0.05}Mn_{0.95}]O_2$ powders were synthesized using a sol-gel method with glycolic acid as chelating agent. Sodium acetate ($NaCH_3CO_2$, Aldrich), manganese acetate ($Mn(CH_3COO)_2{\cdot}4H_2O$, Acros Organics) and nickel acetate ($Ni(CH_3COO)_2{\cdot}4H_2O$, Aldrich) salts were used as starting materials. $NaCH_3CO_2$, $Mn(CH_3COO)_2{\cdot}4H_2O$ and $Ni(CH_3COO)_2{\cdot}4H_2O$ salts with a cationic ratio of Na : Ni : Mn = 0.7 : 0.05 : 0.95 were dissolved in distilled water, and added drop wise to a continuously stirred aqueous solution of glycolic acid. The molar ratio of glycolic acid to total metal ions was unity. The pH of the solution was adjusted in the range of 7-8 by adding ammonium hydroxide. The resultant solution was evaporated at 70-80 °C until a transparent sol was obtained. As the water evaporated further, the sol turned into a viscous transparent gel. The resulting gel precursors were decomposed at 400 °C for 5h in air to eliminate the organic substances. The decomposed powders were calcined at 600 °C for 12 h in air.

The prepared precursor, $Na_{0.7}[Ni_{0.05}Mn_{0.95}]O_2$ powders, was introduced into a mixed solution of hexanol and lithium

bromide. The ion exchange of Na for $Na_{0.7}[Ni_{0.05}Mn_{0.95}]O_2$ with Li was carried out at 160 °C for 8 h in solution in a batch reactor equipped with a reflux condenser to prepare $Li_{0.7}[Ni_{0.05}Mn_{0.95}]O_2$. After the reaction, the solution was filtered using vacuum suction filtering equipment, and the remaining powder was washed with water. The washed powder was dried at 180 °C for one day in a vacuum oven.

Powder X-ray diffraction (XRD, Rigaku, Rint-2000) using Cu Kα radiation was employed to characterize the structural properties of as-prepared powders and cycled electrodes. Rietveld refinement was then performed on the XRD data to obtain the lattice constants. The contents of lithium, nickel, and manganese were measured using the inductively coupled plasma (ICP) method by dissolving the powders in dilute nitric acid. Measurement for the average oxidation state of manganese was carried out by potentiometric titration.

The method is based upon the titration of manganese (II) ions with permanganate in neutral pyrophosphate solution:

$$4Mn^{2+} + MnO_4^- + 8H^+ + 15H_2P_2O_7^{2-} = 5Mn(H_2P_2O_7)_3^{3-} + 4H_2O$$

The manganese (III) pyrophosphate complex was an intense reddish-violet, consequently the titration was performed potentiometrically. A bright platinum indicator electrode and a saturated calomel reference electrode were used. The change in potential at a pH between 6 and 7 is large (about 300 millivolts). The potential of the platinum electrode quickly became constant after each addition of the potassium permanganate solution, thus permitting direct titration to almost the equivalence point and reducing the time required for a determination to less than 10 minutes. With relatively pure manganese solutions, a sodium pyrophosphate concentration of 0.2-0.3 M, and a pH between 6 and 7, the equivalence point potential was $+0.47 \pm 0.02$ volt compared with the saturated calomel electrode. At a pH above 8 the pyrophosphate complex is unstable and this method cannot be used.[18]

For the fabrication of the electrode, the $Li_{0.7}[Ni_{0.05}Mn_{0.95}]O_2$ powders (10 mg) were added to mixed carbon black and polytetrafluoroethylene (PTFE) (6 mg), and pressed onto stainless Exmet. The cell consisted of a cathode and a lithium metal anode separated by a porous polypropylene film. The electrolyte used was a 1 : 1 mixture of ethylene carbonate (EC) and dimethyl carbonate (DMC) containing 1 M $LiBF_4$ by volume. The charge-discharge test was performed galvanostatically at a current density of 0.25 mA cm^{-2}, with cutoff potentials of 2.4 to 4.5 V (*vs*. Li/Li^+). Cyclic voltammetry was carried out using a Potentiostat at a scan rate of 200 $\mu V\ s^{-1}$.

Results and Discussion

The Rietveld refinement of the prepared $Li_{0.7}[Ni_{0.05}Mn_{0.95}]O_2$ powders is shown in Figure 1. The as-prepared powder was confirmed to have O3 structure with space group Rm. The calculated pattern agrees quite well with the observed one.[16]

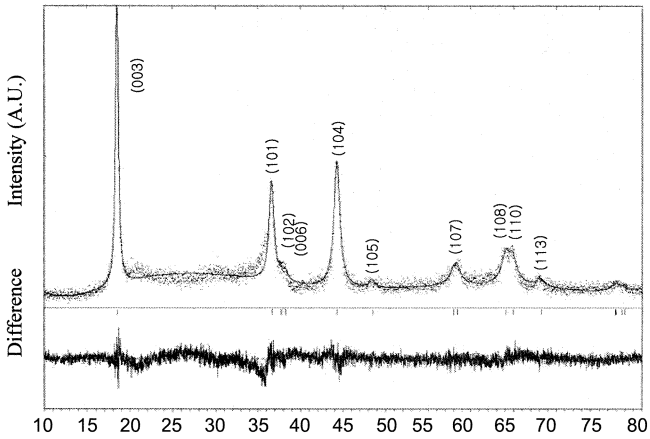

Figure 1. XRD pattern and Rietveld refinement of the O3-$Li_{0.7}[Ni_{0.05}Mn_{0.95}]O_2$ powders.

Though it was difficult to distinguish layered structures from spinel structures due to similarity of the patterns for the materials, we determined that this pattern manifests the layered structure, as is evident from the presence of the split of the (108) (110) peaks at around 65°. In contrast, the spinel structure shows the (108) (110) peaks having merged into a broad peak.[19] We observed that the peak at $2\theta = 16°$ resulting from the initial layered sodium manganese phase disappeared, which indicates that the ion exchange is almost complete. The lattice constants, a and c, of a hexagonal unit cell was calculated by Rietveld refinement from the X-ray diffraction data to be 2.870 and 14.304 Å, respectively. The measured c/a ratio of the powders is 4.98, indicating the formation of hexagonal phase. Figure 2. shows XRD patterns for the samples calcined at different temperatures. As seen in Figure 2, the sample calcined at 600 °C (Figure 2(c)) shows the split of the (108) (110) peaks at around 65°, but there are no peak splits around 65° in the samples calcined at 400 °C (Figure 2(a)) and 500 °C (Figure 2(b)). We concluded that the samples calcined below 600 °C might

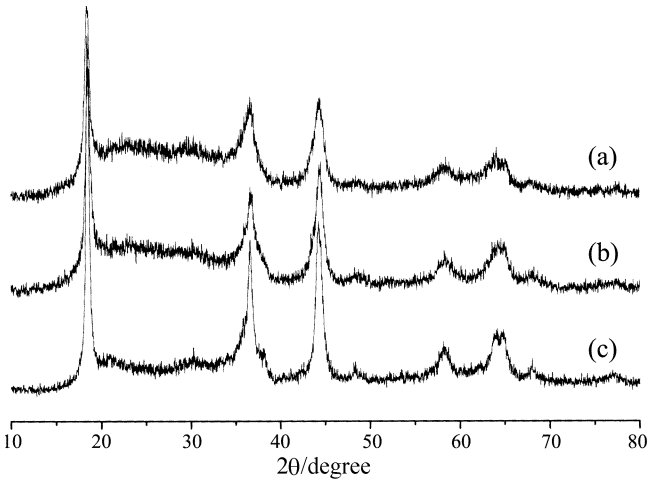

Figure 2. XRD patterns for the samples calcined at various temperature. (a) 400 °C, (b) 500 °C and (c) 600 °C.

increase the formation of cubic phase in the host material, resulting in a degradation of electrochemical performance. The inductive coupled plasma (ICP) analyzed data showed that the real composition was $Li_{0.706}$ $[Ni_{0.053}Mn_{0.95}]O_2$. The average oxidation state of manganese in the material was 3.38, which was measured by a potentiometric titration method reported in the literature.[18] This value is very similar to the theoretical average oxidation state of manganese, 3.37.

Figure 3 shows the discharge capacity for the $Li/Li_{0.7}$-$[Ni_{0.05}Mn_{0.95}]O_2$ cell at room temperature. The cycling was carried out at a constant current density of 0.25 mA cm^{-2} and between potential limits of 2.4-4.5 V. This cell initially delivers a discharge capacity of 163 mA h g^{-1}, which rapidly increases to about 190 mA h g^{-1} after the 5th cycle and retains 97% of the 5th capacity after the 30th cycle. Shao-Horn and co-workers report that the layered Li_xMnO_2 electrodes show greater stability compared with normal $Li_y[Mn_2]O_4$ spinel electrodes, which is attributed to the presence of $Li_{1+x}Mn_{2-z}O_4$ spinel domains ($0 < z < 0.33$) in the composite electrode structure.[20] Evidence suggests that the increment of the initial discharge capacity may be associated with the activation of the cathode material. The voltage profiles for the material are also displayed in Figure 4. The first discharge curve showed a relatively featureless voltage profile. However, with continued cycling, the plateau in 4 V region appeared and the discharge voltage profiles showed two distinct plateaus at around 4 and 3 V, with a sharp slope between the two plateaus. Although the 4 V plateau did not evolve with cycling, the voltage drop between the two plateaus increased. This profile resembles that observed for a spinel-type manganese oxide structure, where the 4 V plateau relates to the insertion of lithium into tetrahedral site, and the 3 V plateau relates to insertion into octahedral site.[21] Research has established that layered materials with small amounts of Al and Co substitution transform to spinel-like phase during cycling.[21,22] Recently,

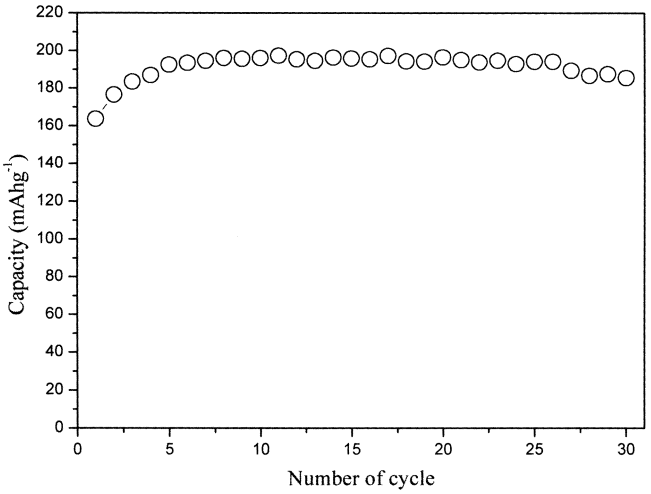

Figure 3. Specific discharge capacity of a $Li_{0.7}[Ni_{0.05}Mn_{0.95}]O_2$ cathode as function of cycle number during expanded cycling at room temperature.

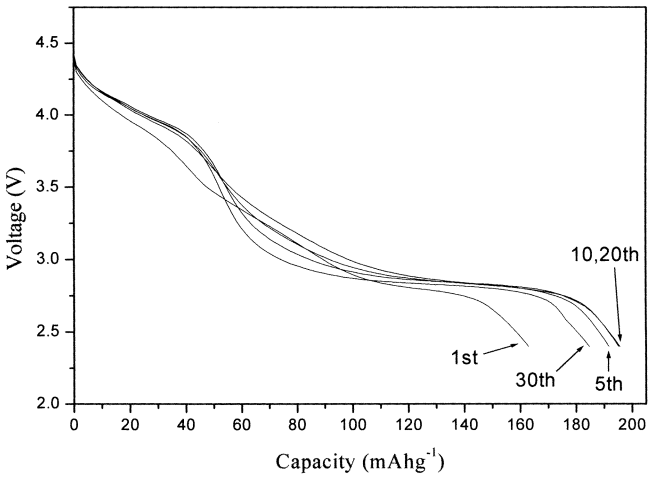

Figure 4. Cycling charge-discharge curves for $Li/Li_{0.7}[Ni_{0.05}$-$Mn_{0.95}]O_2$ cell in the voltage range of 2.4-4.5 V.

Quine and co-workers reported that layered $Li_xNi_{0.05}Mn_{0.95}O_2$ with the O3 (α-$NaFeO_2$) structure delivers a high capacity of 220 mA h g^{-1} in the voltage range 2.4-4.5 V; however, the cycled electrode transforms to a spinel-like structure after scores of cycling.[23] This result indicates that the cathode materials transform to spinel during cycling, although the transformation to spinel evolves slowly.

The investigation of $Li_{0.7}[Ni_{0.05}Mn_{0.95}]O_2$ compared with normal $LiMn_2O_4$ spinel synthesized by our laboratory was carried out using cyclic voltammogram. Examination of the cyclic voltammogram for layered compound in Figure 5, reveals the presence of only one reduction peak at 3.9 V up to the 2nd cycle. After the 3rd cycle, another reduction peak gradually grows at 4.1 V, indicating slow transformation to spinel phase. The cyclic voltammograms for $Li_{0.7}[Ni_{0.05}$-

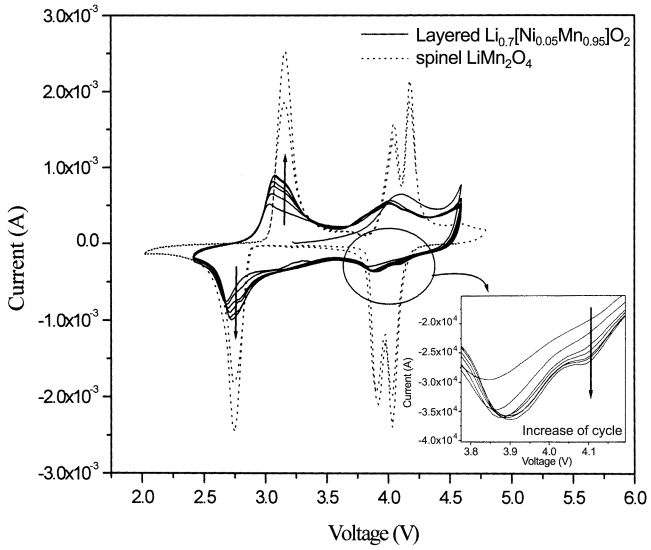

Figure 5. Cyclic voltammogram of layered $Li_{0.7}[Ni_{0.05}Mn_{0.95}]O_2$ and spinel $LiMn_2O_4$ measured at 200 μV s^{-1}. The C.V. data of layered $Li_{0.7}[Ni_{0.05}Mn_{0.95}]O_2$ electrode, highlighting the 4 V region, are displayed in the inset of the Figure 5.

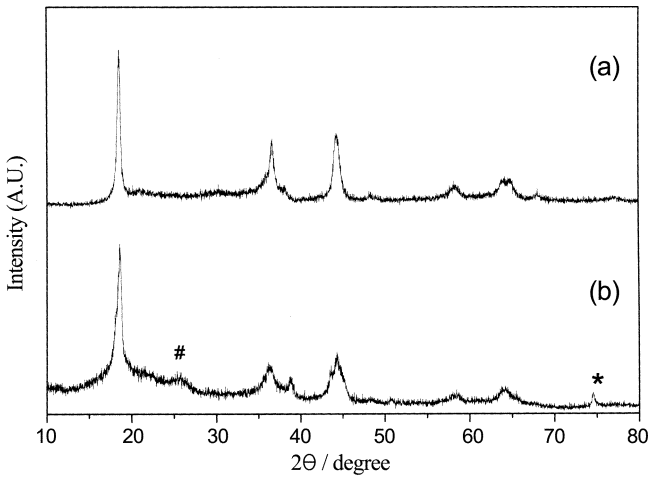

Figure 6. XRD patterns of layered manganese. (a) $Li_{0.7}[Ni_{0.05}Mn_{0.95}]O_2$ as-prepared powders (b) $Li_{0.7}[Ni_{0.05}Mn_{0.95}]O_2$ electrode after 30 cycles.

$Mn_{0.95}]O_2$ compound, highlighting the 4 V region, are displayed in the inset of the Figure 5. The arrows show the direction of progress of cyclic voltammograms, which proves the activation of cathode materials in Figure 3.

To investigate the structural change of the $Li_{0.7}[Ni_{0.05}Mn_{0.95}]O_2$ during cycling, the cycled electrode previously used for the capacity cycle test was characterized with XRD, where the sample was analyzed in the fully discharged state (2.4 V). The results are shown in Figure 6(b). For comparison, data for as-prepared $Li_{0.7}[Ni_{0.05}Mn_{0.95}]O_2$ powders is also presented in Figure 6(a). When comparing XRD patterns of the cycled $Li_{0.7}[Ni_{0.05}Mn_{0.95}]O_2$ with that of as-prepared, no difference could be found in the position of the characteristic peaks, although the cycled electrode shows somewhat low crystallinity. Difficulty is encountered in distinguishing between layered and spinel phases, using X-ray diffraction pattern, due to the similarity of their diffraction patterns. The distinct differences, marked by # and * in Figure 6, are binder and stainless Exmet, respectively. The c/a ratio of the as-prepared powders has an initail value of 4.98 and then it changes to 4.93 after the 30th cycle. Although we could not find any distinct differences in the position of characteristic peaks between the as-prepared powder and cycled electrode, the change of the c/a ratio suggests that the cathode material slowly converted to spinel on cycling because the c/a ratio of 4.899 in hexangonal symmetry is equivalent to a cubic unit cell. This result reinforces the conclusion of the voltage profile studies and the cyclic voltammograms.

Conclusion

Layered $Li_{0.7}[Ni_{0.05}Mn_{0.95}]O_2$ material prepared at 600 °C has a O3 type oxygen packing with space group $R\bar{3}m$. After stabilization, this material shows that the capacity is approximately 190 mA h g^{-1}, with the excellent cycleability in the 2.4-4.5 V range. The voltage profile of $Li_{0.7}[Ni_{0.05}Mn_{0.95}]O_2$ and the cyclic voltammogram data allow us to determine that the $Li_{0.7}[Ni_{0.05}Mn_{0.95}]O_2$ cell gradually converts to spinel during cycling, although we could not find a distinct difference between as-prepared powder and after cycled electrode in the XRD patterns.

Acknowledgment. This work is supported in part by the Ministry of Information & Communication of Korea ("Support Project of University Information Technology Research Center" supervised by KIPA).

References

1. Thackeray, M. M.; David, P. G.; Bruce, P. G.; Goodenough, J. B. *Mat. Res. Bull.* **1983**, *18*, 461.
2. Ohzuka, T.; Kitagawa, M.; Hirai, T. *J. Electrochem. Soc.* **1990**, *137*, 769.
3. Guyomard, D.; Tarascon, J.-M. *Solid State Ionics* **1994**, *69*, 222.
4. Gummow, R. J. de Kock, A.; Thackeray, M. M. *Solid State Ionics* **1994**, *69*, 59.
5. Amine, K.; Tukamoto, H.; Yasuda, H.; Fujita, Y. *J. Electrochem. Soc.* **1996**, *143*, 1607.
6. Amatucci, G. G.; Schmutz, C. N.; Bylr, A.; Siala, C.; Gozdz, A. S.; Larcher, D.; Tarascon, J.-M. *J. Power Sources* **1997**, *69*, 11.
7. Xia, Y.; Zhou, Y.; Yoshio, M. *J. Electrochem. Soc.* **1997**, *144*, 2593.
8. Huang, H.; Vincent, C. A.; Bruce, P. G. *J. Electrochem. Soc.* **1999**, *146*, 481.
9. Sun, Y.-K. *Electrochemistry Communications* **2001**, *3*, 199.
10. Armstrong, A. R.; Bruce, P. G. *Nature* **1996**, *381*, 499.
11. Vitins, G.; West, K. *J. Electrochem. Soc.* **1997**, *144*, 2587.
12. Tabuchi, M.; Ado, K.; Kobayashi, H.; Kageyama, H.; Masquelier, C.; Kondo, A.; Kanno, R. *J. Electrochem. Soc.* **1998**, *145*, L49.
13. Parant, J. P.; Olazcuaga, R.; Devalette, M.; Fouassier, C.; Hagenmuller, P. *J. Solid State Chem.* **1971**, *3*, 1.
14. Paulsen, J. M.; Thomas, C. L.; Dahn, J. R. *J. Electrochem. Soc.* **1999**, *146*, 3560.
15. Paulsen, J. M.; Thomas, C. L.; Dahn, J. R. *J. Electrochem. Soc.* **2000**, *147*, 861.
16. Paulsen, J. M.; Dahn, J. R. *J. Electrochem. Soc.* **2000**, *147*, 2478.
17. Prerre, A. C. In *Introduction to Sol-Gel Processing*; Kluwer Academic Publishers: 1998; p 6.
18. Jeffery, G. H.; Bassett, J.; Mendham, J.; Denney, R. C. In *Vogel's Textbook of Quantitative Chemical Analysis*, 4th ed.; Longman Scientific & Technical: New York, 1978; p 584.
19. Ohzuku, T.; Ueda, A.; Kouguchi, M. *J. Electrochem. Soc.* **1995**, *142*, 4033.
20. Shao-Horn, Y.; Hackney, S. A.; Armstrong, A. R.; Bruce, P. G.; Gitzendanner, R.; Johnson, C. S.; Thackeray, M. M. *J. Electrochem. Soc.* **1999**, *146*, 2404.
21. Ammundsen, B.; Desilvestro, J.; Groutso, T.; Hassell, D.; Metson, J. B.; Regan, E.; Steiner, R.; Pickering, P. J. *J. Electrochem. Soc.* **2000**, *147*, 4078.
22. Armstrong, A. R.; Robertson, A. D.; Bruce, P. G. *Electrochimica Acta* **1999**, *45*, 285.
23. Quine, T. E.; Duncan, M. J.; Armstrong, A. R.; Robertson, A. D.; Bruce, P. G. *J. Mater. Chem.* **2000**, *10*, 2838.